J Solid State Electrochem (2011) 15:773–779
DOI 10.1007/s10008-010-1153-2

ORIGINAL PAPER

Anode-supported solid oxide fuel cell with electrophoretic deposition-derived electrolyte operated under single-chamber conditions and a methane–air mixture

Ming-Yao Cheng · Ching-Yeh Shiau · Ping-Hung Lin · Jen-Chen Chang

Received: 9 June 2010 / Revised: 19 July 2010 / Accepted: 23 July 2010 / Published online: 2 August 2010

Abstract In this study, samaria-doped ceria ($Sm_{0.2}Ce_{0.8}O_{1.9}$, SDC) thin film is deposited on the Ni-SDC support by employing the electrophoretic deposition technique. Various factors are considered for the deposition of SDC films. The corresponding microstructure of the deposited SDC film is examined and correlated to the electrochemical performance as a single-chamber solid oxide fuel cell (sc-SOFC). It is found that the microstructure of the SDC film mainly relates to the particle size of SDC. After heat treatment, highly dense SDC film is obtained with the deposition condition of 5 g L^{-1} of the SDC suspension (average grain size of SDC, 248 nm), 60 V as the applied potential, and the deposition time of 1 min (18 μm in thickness). For the Ni-SDC/SDC/SSC cell, an open circuit potential of 0.92 V and peak power density of 155 mW cm^{-2} can be obtained at the furnace temperature of 500 °C.

Keywords Solid oxide fuel cell · Samaria-doped ceria · Thin film · Electrophoretic deposition · Anode-supported

M.-Y. Cheng
Graduate Institute of Engineering,
National Taiwan University of Science and Technology,
Taipei 106 Taiwan, Republic of China

C.-Y. Shiau (✉) · P.-H. Lin
Department of Chemical Engineering,
National Taiwan University of Science and Technology,
Taipei 106 Taiwan, Republic of China
e-mail: cyshiau@mail.ntust.edu.tw

J.-C. Chang
Chemical Engineering Division,
Institute of Nuclear Energy Research,
Taoyuan 32546 Taiwan, Republic of China

Introduction

Solid oxide fuel cell (SOFC), one of the candidates for clean energy technologies, is able to deliver high power density for various applications. Compared with other kinds of fuel cells, SOFC has several advantages including flexible fuel used, cheaper materials for each component and higher overall efficiency regarding the combined utilization of the produced power and heat. However, a typical SOFC is operated at a high temperature (900 ~ 1,000 °C) owing to the low ionic conductivity of the yttria-stabilized zirconia electrolyte. A high-temperature operation leads to the fast degradation of electrode microstructure, possible interfacial reaction between electrode and electrolyte, mechanical stress resulting from the differences in thermal expansion coefficients between the components, and sealing difficulty. Furthermore, slow startup and the need of expensive materials for the current collector are not favored. Therefore, intermediate-temperature SOFC (IT-SOFC) operated at the range within 500 ~ 700 °C draws much attention, as it is able to alleviate the problems encountered under a high-temperature operation [1]. To achieve operation at intermediate temperatures, the configuration of a thin electrolyte film on the porous electrode support is one of the promised strategies, which is able to reduce the high ohmic loss resulting from the thick electrolyte [2].

Since the success of Hibino et al., a simple single-chamber design for SOFC (SC-SOFC) has been announced worldwide [3–5]. In SC-SOFC, fuel gas and oxygen are premixed as a stream and introduced into a gas chamber that anode and cathode are exposed to. This approach eliminates the sealing problem encountered in a conventional dual-chamber SOFC in which the anode and cathode chambers are separated. Similarly, the pore-free electrolyte is not required. Various designs of the fuel cell stack

constructed for the SC-SOFC cells can be consequently simple and can easily meet the requirement with less total volume. Furthermore, the energy consumed for the maintenance of the high-temperature operation can be greatly reduced since exothermic partial oxidation of the fuel takes place directly at the anode to heat the local cells [3, 6]. The surprising work done by Shao et al. exhibited a high performance of the thermally self-sustained SC-SOFC without heating from a furnace [7]. Although a lot of benefits can be found for SC-SOFC, good selectivity of the electrodes, anode, and cathode toward fuel oxidation and oxygen reduction reaction may be the main criterion.

An excellent performance of the electrolyte-supported Ni-SDC/SDC/SSC SC-SOFC (SDC, $Ce_{0.8}Sm_{0.2}O_{1.9}$; SSC, $Sm_{0.5}Sr_{0.5}CoO_3$) has been first reported by Hibino et al. with peak power densities of 282 and 231 mW cm^{-2} using ethane and propane, respectively, as the fuels at 450 °C. However, the cell failed to give a reasonable performance with methane as the fuel under the same operation condition almost 0 mW cm^{-2} at 450 °C [3]. Nevertheless, methane is one of the most stable fuels that minimize the gas phase reaction with oxygen. The partial oxidation of methane has been intensively studied for SC-SOFC [3, 8–10]. The poor catalytic activity was attributed to the insufficient catalytic activity of Ni-SDC anode to methane at low temperatures where partial oxidation with oxygen is not able to take place [3, 11]. Hibino et al. have also found that the drawback of methane over the Ni-SDC anode can be improved by the addition of noble metals, such as Pd [11], which is effective for the partial oxidation of methane at low temperatures. With a small amount of Pd, cell performance can be improved from ~ μW cm^{-2} to ~270 mW cm^{-2} at 450 °C [11].

A fast, cost-effective, and easily controllable electrophoretic deposition (EPD) method has been demonstrated in the literature for the fabrication of SOFC, especially for the electrode-supported SOFC [12–21]. A crack-free and highly dense film has been obtained by careful control of the synthesis conditions. However, an investigation on the EPD-derived SOFC cell on single-chamber mode is rare. In this work, we have tried to examine the performance of the anode-supported Ni-SDC/SDC/SSC cell by EPD technique. The parameters for EPD deposition of SDC film on the porous Ni-SDC support are discussed. In addition, the low temperature performance of the fabricated single cell was evaluated under single-chamber mode, which is comparable to the cells operated under dual-chamber mode with either hydrogen or methane as the fuel.

Experimental

Synthesis of raw materials All the chemicals were purchased and used as-received. The electrolyte and cathode materials were synthesized by the citrate-gel method. For the SDC powders, 0.04 mol of $Ce(NO_3)_3{\cdot}6H_2O$ (Acros, 99.5%) and 0.01 mol of $Sm(NO_3)_3{\cdot}6H_2O$ (Acros, 99.9%) were dissolved in 100 mL of de-ionized water. Also, 0.1 mole of citric acid (Acros, 99.5%) was dissolved in 100 mL of de-ionized water followed by dropping into the former metal precursor solution with stirring. The mixed solution was heated in a water bath at 80 °C for the gelation process. When a clear gel was obtained, it was further dried at 140 °C and then heat-treated at 600 °C for 5 h in air. A similar procedure was used for the SSC powders. After drying, the solid gel was heated at 1,000 °C for 5 h in air with a ramping rate of 1 °C min^{-1}.

Preparation of anode support Commercial NiO (Acros, 97%) and the synthesized SDC powders were mixed in ethanol in a weight ratio of 1:1 with zirconia balls in a PE bottle. The ball milling process was continued for 24 h. The powders were then dried and pulverized with a mortar. 0.6 g of the pulverized powders was poured in a mold 16 mm in diameter and uni-pressed under a pressure of 50 MPa. The disk was heated at 750 °C for 6 h at ambient atmosphere with a ramping rate of 1 °C min^{-1}. The calcined disk served as the anode support for the deposition of the SDC film.

Preparation of anode-supported SOFC cell EPD was employed for the deposition of SDC film on the NiO–SDC support. Basically, the process developed by Xu et al. was followed [22, 23]. Firstly, the SDC suspension was prepared with the mixed solvent of acetone and ethanol in a volumetric ratio of 3:1. Proper amount of iodine was added to the mixed solvent. Various concentrations of SDC (3, ~ 10 g L^{-1}) in the mixed solvent were prepared. The suspension by the as-synthesized or the ball-milled SDC was prepared for comparison. The above solvent was ultrasonically treated for a couple of minutes to form the required SDC suspension.

For electrophoretic deposition of SDC film on NiO–SDC support, a stainless steel disk 15.5 mm in diameter and the graphite-bonded NiO–SDC support served as the anode and cathode, respectively. The distance between the two electrodes was fixed to be 10 mm. The two electrodes were immersed in the SDC suspension and a voltage of 60 V was then intended to be applied in between. The deposition process was completed within several minutes (1~3 min). The deposited SDC film on NiO–SDC support was co-fired with a heating program of 5 °C min^{-1} to 1,000 °C and held for 1 h, which was followed by 2 °C min^{-1} to 1,350 °C and held for 12 h.

The SSC cathode was prepared by screen printing. The slurry was prepared with the SSC powders, ethyl cellulose, and α-terpineol in a weight ratio of 2:1:1. The above mixture was ball-milled for 24 h to obtain homogeneous slurry. The slurry was applied on the SDC film by screen printing, followed by heating at 1,100 °C for 5 h.

Characterization The phase confirmation of the raw materials was characterized by X-ray diffraction (XRD) technique using an X-ray diffractometer (Rigaku D/Max-RC, Japan) operated under Cu Kα radiation (1.5406 Å) at 40 kV and 100 mA [24]. The materials are pelletized for XRD characterization. The particle size distribution of the SDC powders was determined with a laser light scattering system (Photal DLS-7000). The microstructures and thickness of the electrode and the electrolyte were characterized by a scanning electron microscope (SEM, JEOL JSM-6500F). For electrochemical characterization, Ag net and Au wires were attached to the electrode surfaces for current collection. The impedance of the SOFC cell was characterized using an electrochemical system combining a Solartron 1260 Frequency Response Analyzer and a Solartron 1286 Potentiostat. The applied frequency ranged from 10^5 to 10^{-1} Hz with the signal amplitude of 20 mV. The fuel cell performance was characterized at the furnace temperature of 500 °C. Prior to characterization, the anode was reduced at 600 °C for 6 h with a ramping rate of 5 °C min^{-1}. The atmosphere was controlled with a mixture gas of H_2 and Ar in a volumetric ratio of 1:9 and a flow rate of 100 mL min^{-1}. After reduction, the furnace temperature was reduced to the target temperature for the fuel cell characterization. The reactant gas was composed of methane and air premixed in a ratio of 3:7. The total flow rate was fixed at 300 mL min^{-1}.

Results and discussion

First of all, phase confirmations of the synthesized SDC and SSC powders are examined by XRD and shown in Fig. 1. Figure 1 clearly indicates that the cubic fluorite structure of the synthesized SDC powders and the pure perovskite structure of the synthesized SSC powders can be identified with the JCPDS file (JCPDS No. 75-0158). No impurities are observed in the acquired XRD pattern [25].

The deposition behaviors of the SDC thin film by EPD may reflect on its quality after heating. The amount of iodine in the mixed solvent was firstly discussed for the EPD process. Chen et al. indicates that the addition of iodine in an acetone–ethanol mixed solvent may produce protons by the substitution reaction [26]:

$$CH_3COCH_3 + 2I_2 \rightleftarrows ICH_2COCH_2I + 2H^+ + 2I^- \quad (1)$$

$$CH_3CH_2OH + I_2 \rightleftarrows ICH_2CH_2OH + H^+ + I^- \quad (2)$$

The produced protons are able to adsorb on the surface of the particles. With proper voltage applied, the charged particles would move toward the cathode side in the EPD system. Figure 2 exhibits the effect of iodine concentration

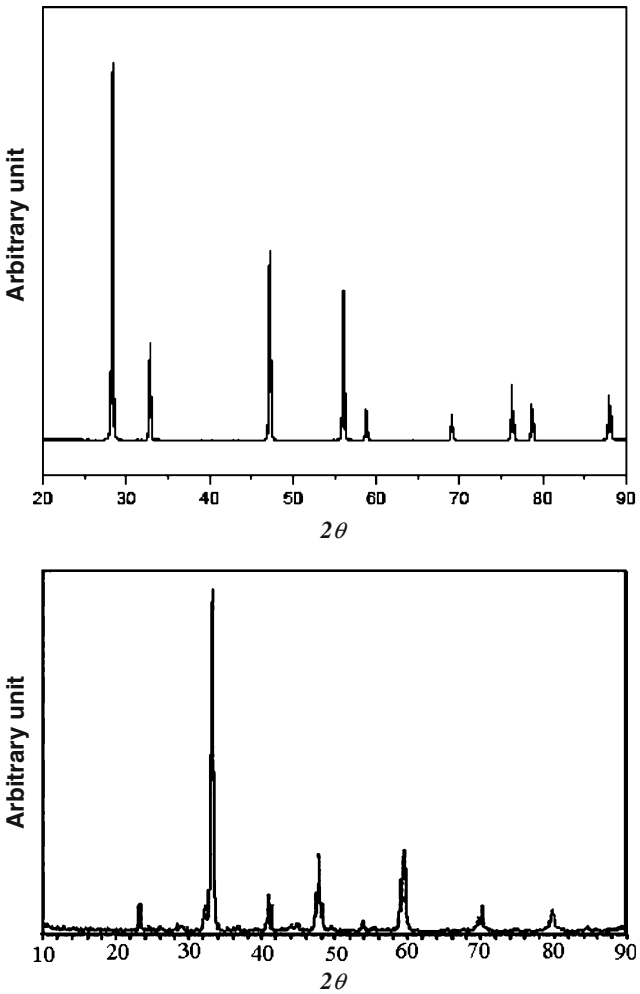

Fig. 1 XRD patterns for the synthesized SDC and SSC powders

in an acetone–ethanol mixed solvent to the deposited weight of SDC (weight change of NiO–SDC anode support before and after EPD). The applied voltage is 60 V and held for 30 s for all the EPD processes with the as-synthesized SDC powders (320 nm) as the suspension feedstock. The maximum deposited weight appears at the iodine concentration of 0.6 g L^{-1}, which indicates the saturation of protons on the SDC particle surface in this work. A higher iodine concentration in the solvent implies a higher percentage of free protons. Therefore, the competition between free protons and charged SDC particles during the EPD process would result in fewer charged particles deposited onto the NiO–SDC support (cathode side). Further, evolution of H_2 may take place as well, which would lead to porous SDC film.

The effect of various SDC concentrations (3, 4, 5, or 10 g L^{-1}, 320 nm SDC) in the suspension was investigated for EPD process. During the process, the applied voltage was fixed at 60 V and the iodine concentration was 0.6 g L^{-1}. After 3-min deposition followed by heating at

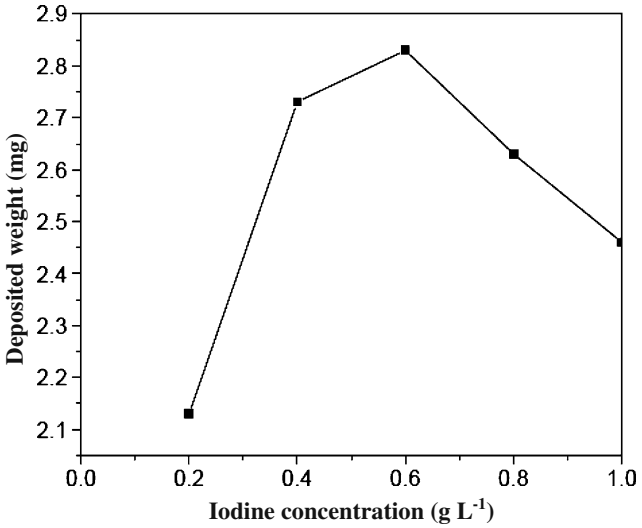

Fig. 2 Effect of iodine concentration on the amount of deposited SDC by EPD technique

1,350 °C, the microstructure of the SDC films were characterized by SEM, the images of which are shown in Fig. 3. It is worth to note that all the deposited films are porous, which indicates that the density of the film may not be associated with the suspension concentration. Further, no linear relationship between the thickness of the deposited film and the SDC concentration is observed. For the SDC films deposited with suspension of 5 or 10 g L^{-1}, the thickness is about 37 μm. However, 32 μm is obtained for the suspension of 3 or 4 g L^{-1}. It is proposed that the insufficient quantities of iodine in the mixed solvent result in the partial precipitation of the suspension.

It is clear that the porous SDC film cannot be avoided even after a high-temperature treatment (Fig. 3). Therefore, ball-milling process was introduced to obtain uniform and fine SDC particles. Figure 4 shows the particle size distribution of the synthesized SDC powders before and after the balling-milling process by laser light scattering technique. Obviously, the size distribution of the as-synthesized SDC powders is boarder than that of the ball-milled one. The average particle size for the as-synthesized SDC powders is about 320 nm (Fig. 4a) and is reduced to 248 nm after ball-milling for 24 h (Fig. 4b). The effectiveness of a simple ball-milling process can thus be realized. Later, the suspension by the ball-milled SDC powders was prepared for the EPD process. The iodine and ball-milled SDC concentrations are fixed to 0.6 and 5 g L^{-1}, respectively. The EPD process was performed for 1 min with an applied voltage of 60 V, which is followed by heating at 1,350 °C. From Fig. 5, the resulting film is highly dense with the thickness of 18 μm. By comparing the results shown in Figs. 4 and 5, it is clear that uniform and fine particles are the key factors for a highly dense film by EPD process.

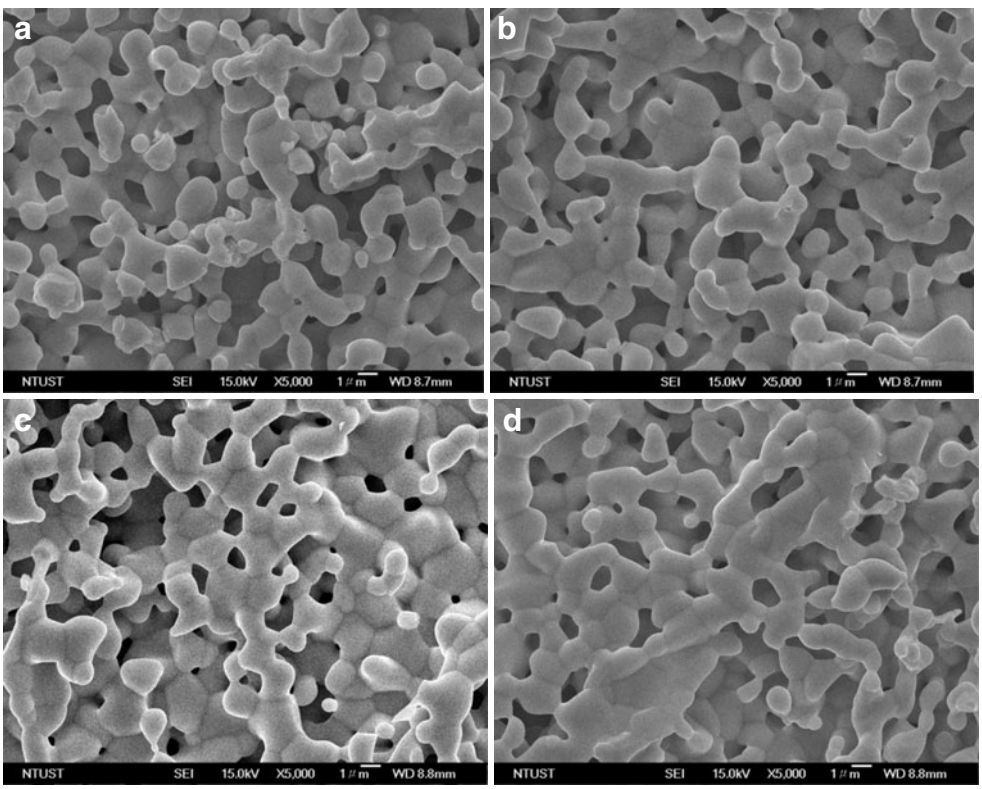

Fig. 3 SEM images of sintered SDC films prepared by EPD technique (applied voltage, 60 V; deposition time, 3 min) with various SDC (320 nm) concentrations in the suspension (**a** 3, **b** 4, **c** 5, and **d** 10 g L^{-1})

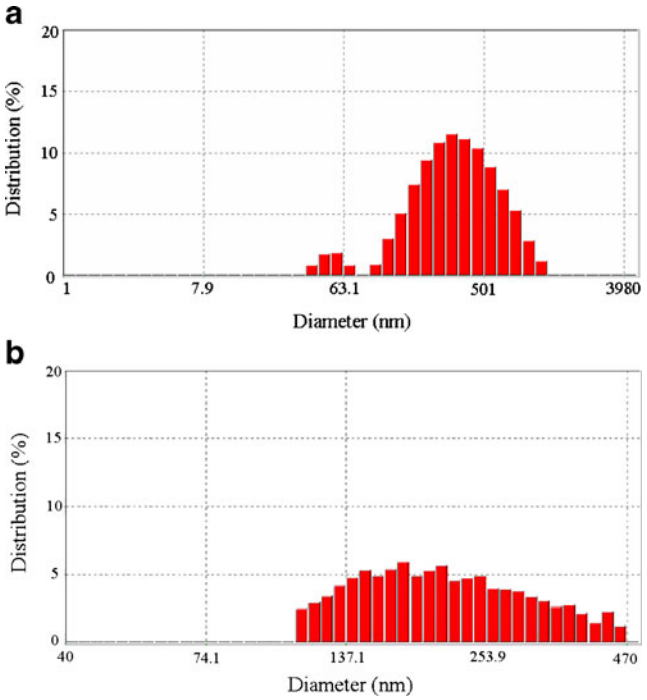

Fig. 4 Particle size distributions of the **a** as-prepared (denoted as 320 nm) and **b** 24-h ball-milled (denoted as 248 nm) SDC powders using laser light scattering technique

The impedance of the Ni-SDC/SDC/SSC cell was analyzed by two-electrode configuration. A comparison of the SDC thin films with 248 and 320 nm SDC powders is made and shown in Fig. 6. For impedance analysis, the operating temperature of the cell is 500 °C in air. Obviously, the impedance for the cell with the thin film by 248 nm SDC powders (34 μm) is much smaller than that by the 320-nm ones (37 μm). The thickness of the electrolyte film should contribute to the resulting impedance, but the electrolyte film by SDC-320 exhibits only

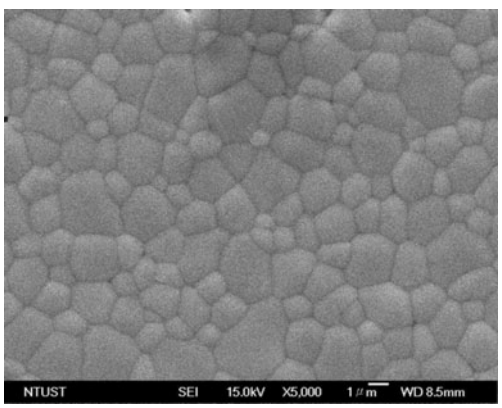

Fig. 5 SEM images of sintered SDC films prepared by EPD technique (applied voltage, 60 V; deposition time, 1 min) with SDC (248 nm) concentration of 5 g L^{-1} in the suspension

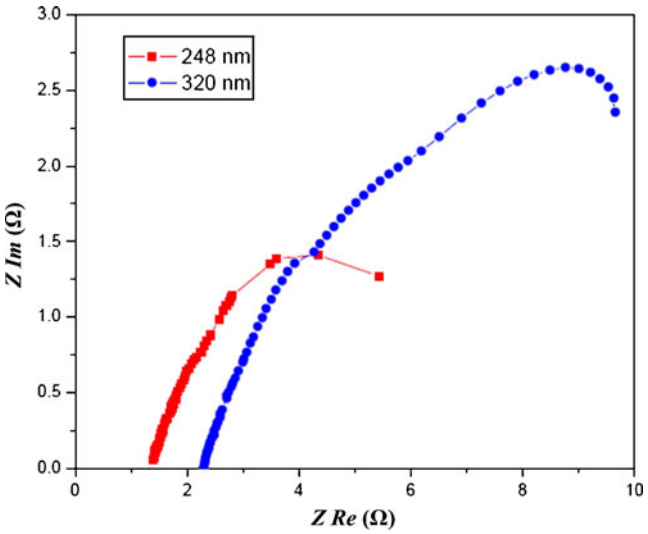

Fig. 6 Comparison of AC impedances for the Ni-SDC/SDC/SSC cells using 248 and 320 nm SDC powders for the electrolyte thin film

10% thicker than that by SDC-248. Considering the electrolyte impedance from the spectra, the impedance of the electrolyte film by SDC-320 is 2.3 Ω (the intercept of the spectrum and *X*-axis), which is 64% higher than that by SDC-248 (1.4 Ω). The result indicates that there should be other factors influencing the electrolyte impedance rather than thickness. Clearly, the two electrolytes exhibit large difference in their densities, which can be evidenced from the corresponding SEM images (Figs. 3 and 5). Usually, the porous electrolyte film leads to higher ionic transport resistance between grains, which could be the main reason for the higher impedance of the electrolyte film by SDC-320.Although porous electrolyte may work in SC-SOFC, higher impedance would hinder the oxygen transport and subsequently reduce the performance.

The polarization curve of the Ni-SDC/SDC/SSC cell was examined under a mixed methane–air (3:7) atmosphere. Comparing two cells with the SDC thin films deposited, respectively, by 248 and 320 nm SDC powders at 500 °C (Fig. 7, 10 g L^{-1}), the former one shows a slightly higher open circuit potential (OCP) than the later one (0.82 to 0.8 V). Interestingly, the former cell exhibits a much higher peak power density than the later one (135 to 115 mW cm^{-2}). It is possibly owing to the higher impedance of the SDC thin film derived from the 320 nm SDC powders, which the higher ohmic loss can realize under high current output. The results obtained herein are quite different from the literature, wherein the electrolyte-supported Ni-SDC/SDC/SSC cell only can deliver peak power density of ~μW cm^{-2} with OCP of 0.11 V at 500 °C with a methane–air mixture [8]. It implies that the assistance of noble metal for the partial oxidation of methane proposed in the literature can be eliminated with

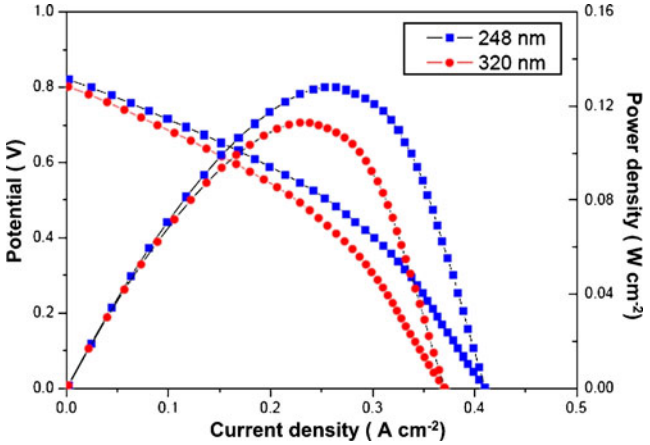

Fig. 7 Comparison of the cell polarization curves at 500 °C with electrolyte films prepared with 248 and 320 nm SDC powders

the anode-supported configuration. We propose that the possible reasons for the high performance are the higher number of active sites for partial oxidation of methane as provided by the anode support and the thin SDC film. The anode-supported SOFC is composed of much more nickel particles than the electrolyte-supported SOFC does. The partial oxidation of methane takes place on the nickel surface in the presence of oxygen. Even the catalytic ability of nickel is less than that of the commonly used noble metals, e.g., Pd, the much higher numbers of nickel particles in the anode-supported SOFC compensate for the poor catalytic ability. For single-chamber SOFC, the heat released from the exothermic partial oxidation is able to increase the local temperature of the SOFC cell, which facilitates the reaction rate of the electrocatalytic oxidation of methane. Furthermore, the thickness of the electrolyte film produced by the EPD method is much thinner than that for a common electrolyte-supported SOFC. Therefore, the local temperature of the electrolyte film may be higher than that of electrolyte-supported SOFC, resulting in higher ionic conductivity. The higher number of active sites provided by nickel particles leads to a higher local temperature of the SOFC cell and, subsequently, the electrocatalytic ability of an electrode and the higher ionic conductivity of an electrolyte film improve the SOFC performance.

In the previous paragraphs, it is mentioned that the thickness of the deposited SDC thin film is similar with the suspension concentration of 5 and 10 g L^{-1}. However, the exhibited performance is not identical. The polarization curves of the cell with the suspension concentration of 5 g L^{-1} are shown in Fig. 8. The highest OCP of 0.92 V with the maximum peak power density of 155 mW cm^{-2} is obtained for the cell operated at 500 °C. It is proposed that the densities of the SDC films prepared with different suspension concentrations may change after sintering, which results in a difference in the corresponding electrochemical performance. It is believed that the charge density on the SDC particle surface may impact the quality of the electrophoretic-deposited film. With the same iodine concentration, a higher SDC concentration in the suspension solution results in a lower charge density on the SDC particles. Therefore, the driving force for the SDC particles in the suspension of higher SDC concentration would be smaller, which probably leads to the deposited film being less compact. Furthermore, it can be noticed that the low temperature performance is comparative to the results shown in the literature without usage of noble metals [27–31], which demonstrates the EPD technique for application in the development of the Ni-SDC/SDC/SSC cell. However, the SDC thin film behaves as the n-type semiconductor at the furnace temperature higher than 500 °C, which leads to lower OCP of the cell.

Conclusion

In this work, Ni-SDC/SDC/SSC cell was prepared and operated under the single-chamber conditions with methane–air mixture. It was found that the importance of the proper iodine concentration and small and uniform SDC powders for EPD suspension is manifest to obtain a high-quality SDC film. Further, the results exhibit the anode-supported configuration as being able to overcome the poor catalytic ability of methane partial oxidation reaction on Ni-SDC anode, in which the aid of noble metals can be eliminated.

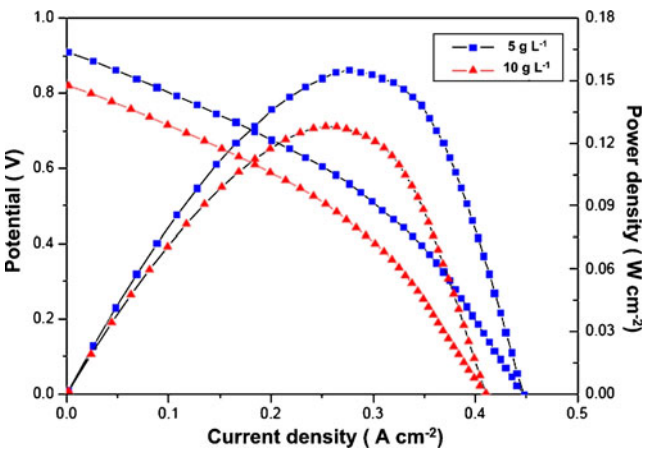

Fig. 8 Comparison of the cell polarization curves at 500 °C with electrolyte films prepared with different suspension concentrations of 248 nm SDC powders

Acknowledgement The authors gratefully acknowledge the financial supports from the National Science Council of the Republic of China under Contract No. NSC-97-2221-E-011-056.

References

1. Antepara I, Villarreal I, Rodríguez-Martínez LM, Lecanda N, Castro U, Laresgoiti A (2005) J Power Sources 151:103
2. Will J, Mitterdorfer A, Kleinlogel C, Perednis D, Gauckler LJ (2000) Solid State Ionics 131:79
3. Hibino T, Hashimoto A, Inoue T, Tokuno J, Yoshida S, Sano M (2000) Science 288:2031
4. Hibino T, Ushiki K, Kuwahara Y (1996) Solid State Ionics 91:69
5. Hibino T, Kuwahara Y, Wang S (1999) J Electrochem Soc 146:2821
6. Yano M, Tomita A, Sano M, Hibino T (2007) Solid State Ionics 177:3351
7. Shao Z, Haile SM, Ahn J, Ronney PD, Zhan Z, Barnett SA (2005) Nature 435:795
8. Shao ZP, Kwak C, Haile SM (2004) Solid State Ionics 175:39
9. Napporn TW, Jacques-Bedard X, Morin F, Meunier M (2004) J Electrochem Soc 151:A2088
10. Suzuki T, Jasinski P, Petrovsky V, Anderson HU, Dogan F (2005) J Electrochem Soc 152:A527
11. Hibino T, Hashimoto A, Yano M, Suzuki M, Yoshida S, Sano M (2002) J Electrochem Soc 149:A133
12. Besra L, Liu M (2007) Prog Mater Sci 52:1
13. Zhitomirsky I, Petric A (2004) J Mater Sci 39:825
14. Besra L, Zha S, Liu M (2006) J Power Sources 160:207
15. Jia L, Lü Z, Huang X, Liu Z, Chen K, Sha X, Li G, Su W (2006) J Alloys Compd 424:299
16. Matsuda M, Hosomi T, Murata K, Fukui T, Miyake M (2007) J Power Sources 165:102
17. Nakayama S, Miyayama M (2007) Key Eng Mater 350:175
18. Jia L, Lü Z, Huang X, Liu Z, Zhi Z, Sha X, Li G, Su W (2007) Ceram Int 33:631
19. Hosomi T, Matsuda M, Miyake M (2007) J Eur Ceram Soc 27:173
20. Bozza F, Polini R, Traversa E (2009) Electrochem Commun 11:1680
21. Zunic M, Chevallier L, Deganello F, D'Epifanio A, Licoccia S, Bartolomeo ED, Traversa E (2009) J Power Sources 190:417
22. Xu Z, Rajaram G, Sankar J, Pai D (2007) Fuel Cells Bulletin 2007:12
23. Xu Z, Rajaram G, Sankar J, Pai D (2006) Surf Coat Tech 201:4484
24. Shao L, Liu L, Cheng S-X, Huang Y-D, Ma J (2008) J Membr Sci 112:174
25. Song HS, Min JH, Kim J, Moon J (2009) J Power Sources 191:269
26. Chen F, Liu M (2001) J Eur Ceram Soc 21:127
27. Piñol S, Morales M, Espiell F (2007) J Power Sources 169:2
28. Wei B, Lü Z, Huang X, Liu M, Chen K, Su W (2007) J Power Sources 167:58
29. Lin Y, Zhan Z, Liu J, Barnett SA (2005) Solid State Ionics 176:1827
30. Ruiz de Larramendi I, Lamas DG, Cabezas MD, Ruiz de Larramendi JI, Walsoe de Reca NE, Rojo T (2009) J Power Sources 193:774
31. Buergler BE, Siegrist ME, Gauckler LJ (2005) Solid State Ionics 176:1717